

Cell Stem Cell, Volume 2

**Supplemental Data**

**Trophoblast Differentiation Defect**

**in Human Embryonic Stem Cells Lacking**

**PIG-A and GPI-Anchored Cell-Surface Proteins**

Guibin Chen, Zhaohui Ye, Xiaobing Yu, Jizhong Zou, Prashant Mali, Robert A. Brodsky, and Linzhao Cheng



**Table S1.** A partial list of GPI-APs expressed in undifferentiated (Undiff) & differentiated (Diff) human ES cells

Gene Game*	Undiff	Diff	Ratio	Genbank ID	Gene Description
Cripto	46.82	0.19	246.42	NM_003212	Cripto co-receptor or co-ligand; TDGF1
ALPL	6.62	0.81	8.14	X14174	alkaline phosphatase (APase), liver/bone/kidney (tissue non-specific) type
EPHA1	7.87	1.69	4.66	NM_005232	Ephrin A1 ligand; average of two entries (2x)
CD24	46.47	10.29	4.52	X69397	CD24; heat stable or small cell lung carcinoma cluster 4 antigen; 5x
LPL	0.22	0.08 (A)	2.75	BF672975	lipoprotein lipase, 2x
ACHE	0.24	0.09 (A)	2.67	NM_015831	acetylcholinesterase (YT blood group), 2x
GPC4	23.88	10.01	2.38	NM_001448	glypican 4
GFRA2	0.13	0.06 (A)	2.27	NM_001495	GDNF family receptor alpha 2
CNTN1	1.52	0.96	1.58	U07820	contactin 1
EPHA3	0.23	0.15	1.53	AF213460	Ephrin A3 ligand
EPHA4	0.16	0.11	1.53	NM_004438	Ephrin A4 ligand
GFRA1	0.36	0.25	1.43	NM_005264	GDNF family receptor alpha 1
ALPPL2	0.36	0.27	1.34	J04948	alkaline phosphatase, placental-like 2
LY6H	0.39	0.30	1.30	NM_002347	lymphocyte antigen 6 complex, locus H
NTNG1	0.92	0.79	1.16	NM_014917	Netrin G1; extrinsic to plasma membrane, GPI-anchored
PrP	7.30	7.82	1.07	NM_000311	Prion protein
GML	1.07	1.02	1.05	NM_002066	GPI anchored molecule like protein
Thy-1/CD90	15.76	15.98	0.99	AL558479	Thy-1 (CD90) cell surface antigen, 3x
GPC3	3.72	4.03	0.92	L47125	glypican 3
CD59	7.25	8.28	0.88	NM_000611	CD59 antigen; p18-20
EPHA5	0.45	0.52	0.87	L36644	Ephrin A5, ligand
NCAM2	0.36	0.42	0.86	NM_004540	neural cell adhesion molecule 2
NCAM1	0.57	0.65	0.86	AA126505	neural cell adhesion molecule 1
EPHA2	4.48	5.64	0.79	NM_004431	Ephrin A2 ligand
CD48	0.68	0.95	0.72	NM_001778	CD48 antigen
Neuritin	0.46	0.59	0.78	NM_016588	Neuritin/CPG15
GPC1	1.56	2.36	0.66	NM_002081	glypican 1
LY6E	2.19	3.39	0.65	NM_002346	lymphocyte antigen 6 complex, locus E
DAF/CD55	2.30	3.62	0.64	BC001288	decay accelerating factor for complement (CD55), 2x
GFRA3	0.31	0.60	0.51	NM_001496	GDNF family receptor alpha 3
EPHA7	0.46	1.47	0.32	NM_004440	Ephrin A7 ligand
GPC5	0.02 (A)	0.16	0.13	NM_004466	glypican 5
^RGMa	0.03	0.01 (A)	3.02	NM_020211	Repulsive Guidance Molecule A
^RGMb/DRAGON	0.37	0.14	2.49	NM_173670	Repulsive Guidance Molecule A/DRAGON
^RGMc/HFE2	0.02	0.08	0.22	NM_213653	Repulsive Guidance Molecule A/HFE2

\*GPI-APs confirmed by FACS;

A: Absent in gene expression. See Dravid et al. (2005) for more details of gene array analysis;

^: The 3 genes were not included in the U133A chip used above. Instead, the value from a different array analysis using an Agilent chip with H1 hES cells in the presence or absence BMP4 treatment for 10 days.

**Table S2.** Clonal derivation of human ES cells lacking GPI-APs

Cell batch	Numbers of sorted cells/well	Numbers of wells with one or more colonies			
		1 colony	2 colonies	3 colonies	4 colonies
AR1	1 cells/well, 96 wells	0	0	0	0
	5 cells/well, 96 wells	<b>2<sup>1</sup></b>	0	0	0
	10 cells/well, 96 wells	14	2	0	0
AR2	5 cells/well, 96 wells	<b>2<sup>2</sup></b>	0	0	0
	10 cells/well, 96 wells	26	22	2	0

Limiting dilution experiments to achieve clonal hES cells after pro-aerolysin resistance (AR) selection in two independent experiments (AR1 and AR2). After AR selection, undifferentiated human ES cells (SSEA4+) lacking GPI-AP Thy-1/CD90 expression were sorted by FACS and seeded at either 1, 5 or 10 cells per well in a 96-well plate (containing feeder cells). Human ES cells were cultured for 7 days and inspected daily. The observed colonies in each well under each condition were recorded. Human ES cells in 4 wells (**bold**) that contained a single colony from the least number (5) of seeded cells were harvested and expanded. Two independent clones, AR1-c1<sup>1</sup>, and AR2-c1<sup>2</sup>, were derived from one of the only 2 wells that came up a single colony in each batch. The lack of multiple GPI-APs and retaining of undifferentiated marker and morphology are shown in Figure 1.

**Table S3.** Primers used for human genes by conventional (semi-quantitative) RT-PCR

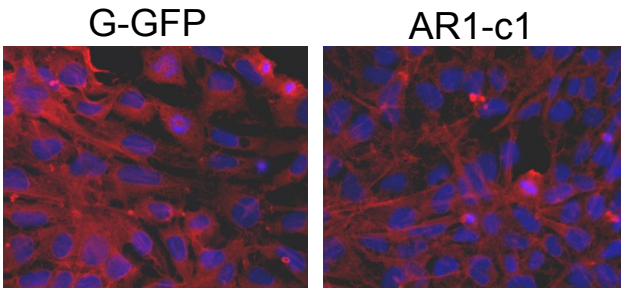
Gene name	Primer Sequences (5'-3')		Product size (bp)
	Sense (upstream)	Anti-sense (downstream)	
PIG-A	ACTGGCGGCCATGGAACTCA	GAGCATCATGGGCCATAGCA	520
Alpha-fetal protein (AFP)	AGCTTGGTGGTGGATGAAAC	TCCAACAGGCCTGAGAAATC	200
CD34	CTGTGTCTCAACATGGCA	GCCTTGATGTCACCTTAGG	298
PAX6	TCCATCAGTTCCAACGGAGAAG	GTGGAATTGGTTGGTAGACTG	337
Musashi (MSI) I	ACAGCCCAAGATGGTGACTC	CCACGATGTCCTC ACTCTCA	191
CG $\alpha$	CAGAATGCACGCTACAGGAA	CGTGTGGTTCTCC ACTTTGA	218
CG $\beta$	GCACCAAGGATGGAGATGTT	GCACATTGACAGCTGAGAGC	314
NANOG	CAGAAGGCCTCAGCACCTAC	ACTGGATGTTCTGGGTCTGG	245
RGMa	CGAGATCTGCCATTACGAGA	GGTCCACACACTCCTGGAAG	260
RGMb/DRAGON #1	TGAGAGCAGCACCTTCC AG	AAGGCCTTGCAAAACTCAGA	247
RGMb/DRAGON #2	GGTGACTGCCAACAGCCAGCC	ACTGCTGGGGAAAATGTGCCA	1098
$\beta$ -Actin	GCTCG TCGTCGACAACGGCTC	CAAACATGATCTGGGTCATCTTCTC	353

**Figure S1. Cripto proteins in AR1-c1 cells were made intracellularly but unable to display**

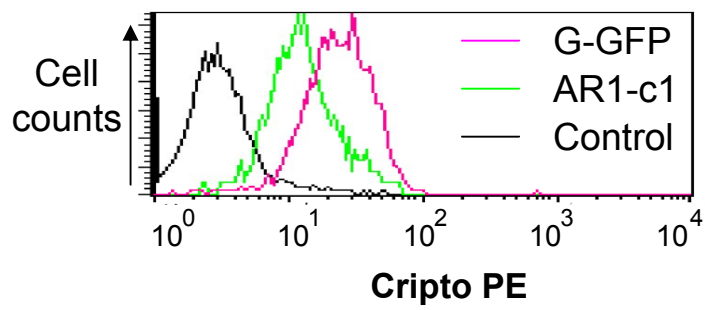
**on cell surface. (a).** Staining for Cripto proteins after G-GFP or AR1-c1 cells were permeabilized. Human ES cells cultured on a feeder-free condition were fixed and treated with NP-40 to permeabilize cells. Un-conjugated mouse monoclonal antibodies recognizing the Cripto peptide were incubated with cells overnight. After wash, the Cripto antibody binding was visualized by an anti-mouse antibody conjugated with Texas Red. Cell nuclei were stained by DAPI. The Cripto peptide was detected both on cell surface and in cytoplasm in G-GFP cells. However, in AR1-c1 cells after permeabilization it was detected (primarily in cytoplasm in an irregular shape). **(b).** FACS analysis of permeabilized G-GFP and AR1-c1 cells by a PE-conjugated anti-Cripto antibody.

# Fig S1

a. Cripto staining of permeabilized cells



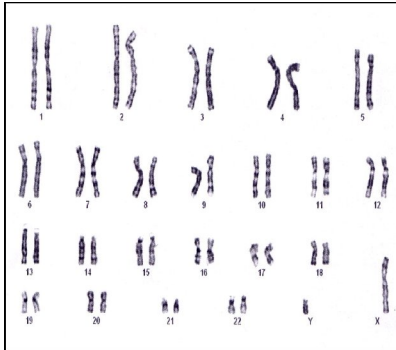
b. FACS analysis of permeabilized cells



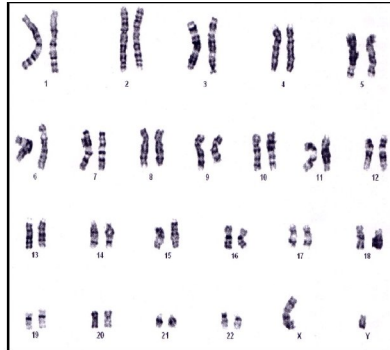
**Figure S2. Representative karyotyping results of G-GFP (parental), AR1-c1 and AR2-c2 human ES cells.**

Fig S2. Karyotyping Assay in undifferentiated ES cells

*a. G-GFP*



*b. AR1-c1*



*c. AR2-c1*

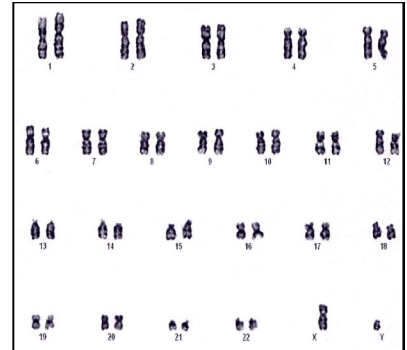
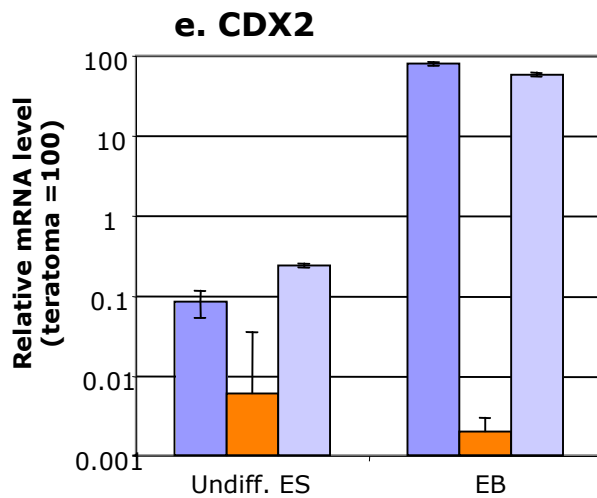
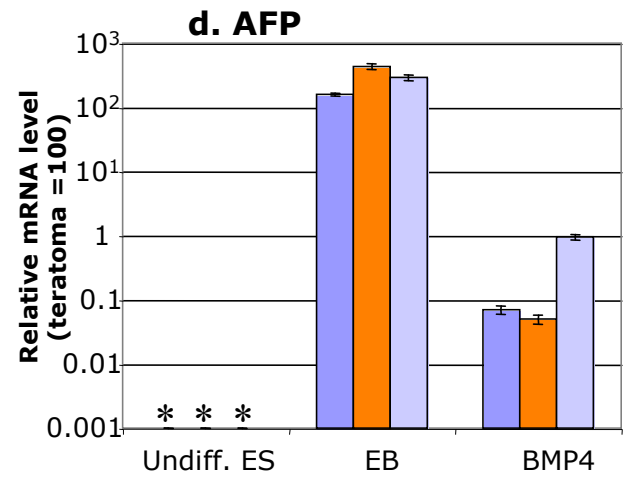
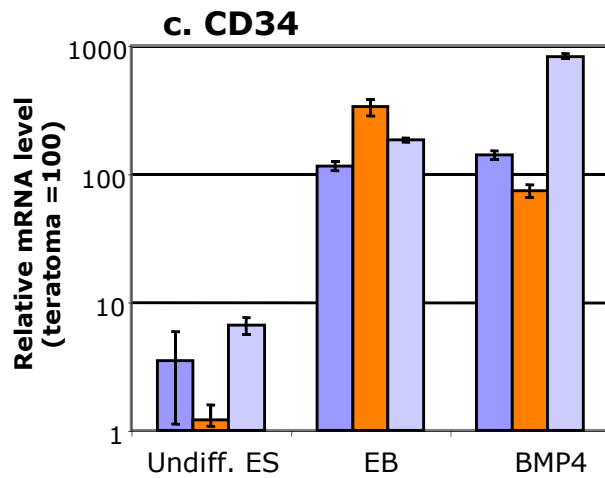
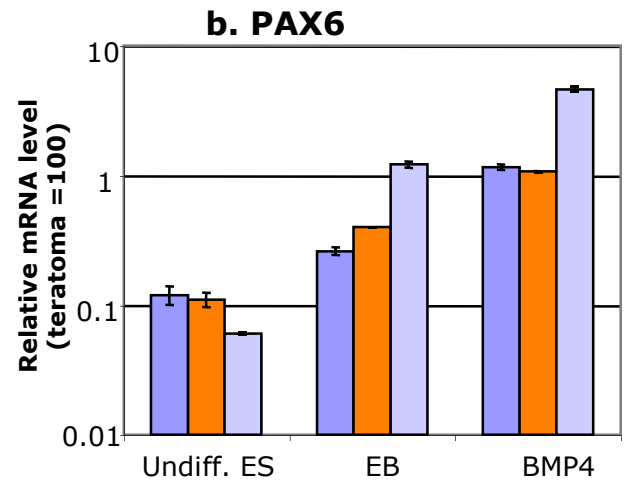
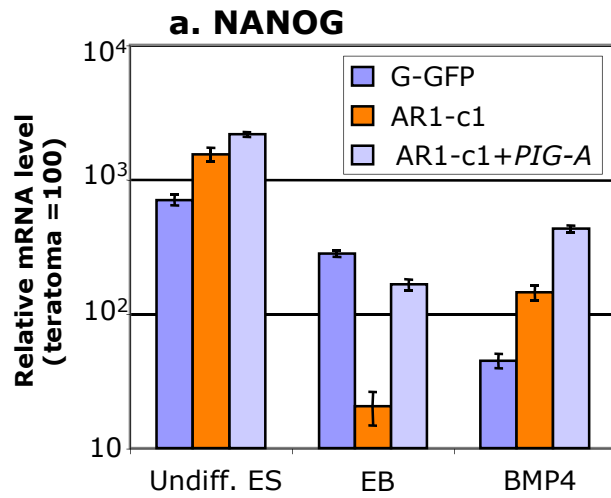




**Figure S3. Quantitative RT-PCR to measure the expression of various marker genes.**

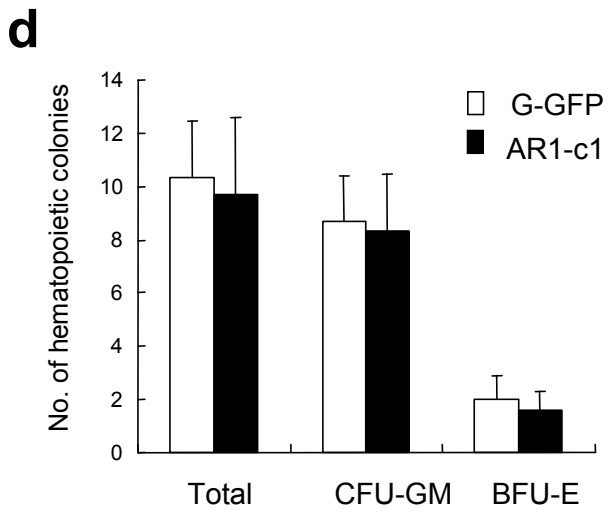
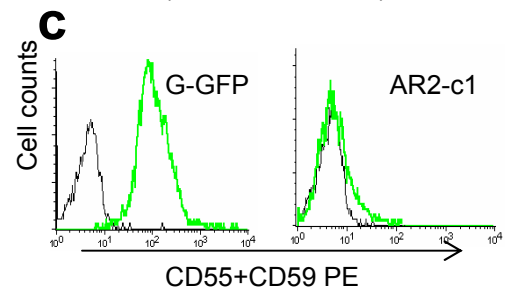
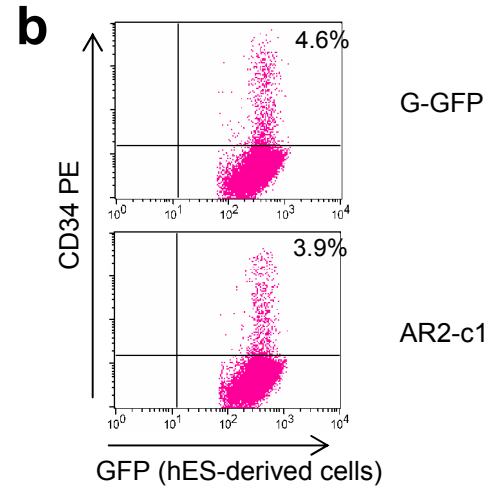
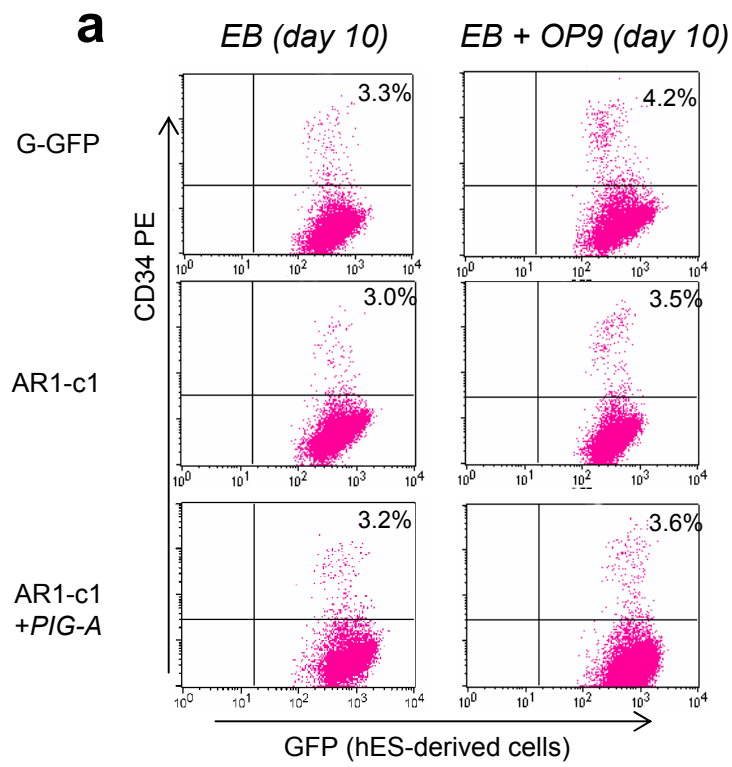
Undifferentiated G-GFP and AR1-c1 hES cells, as well as their differentiated derivatives after embryoid body formation (EB, day 10) or BMP4 induction (BMP4, day 10) were harvested and analyzed for gene expression. The mRNA level is quantified by RT-PCR with specific primers and probes for (a) NANOG, an undifferentiated marker; (b) PAX6, an ectoderm marker; (c) CD34, a mesoderm marker; (d) AFP, an endoderm marker; and (e) CDX2, a trophectoderm/trophoblast marker. The level of  $\beta$ -actin is also measured as an internal control for normalization for each sample. RNA from teratomas derived from the wildtype hES cells was also used as a common reference (defined as 100), since teratomas contain a mixed cell population expressing every gene involved. The relative mRNA level (relative to that in teratoma) is plotted in a log scale. \*, undetectable after 40 cycle PCR.

Fig S3



**Figure S4. The formation of CD34<sup>+</sup> cell and hematopoietic progenitors from PIG-A/GPI-AP deficient hES cells appears normal.** (a) The parental (G-GFP) and AR1-c1 hES cells were allowed to form embryoid bodies (EBs) in suspension for either 5 or 10 days. A half of EB samples were harvested and further cultured with OP9 mouse stromal cells for 5 days. At day 10, cells from both culture conditions, EB (day 10) or EB+OP9 (day 10), were harvested and dissociated for flow cytometric analysis. Human ES cell derivatives, distinguishable from mouse OP9 stromal cells by their GFP expression, were analyzed by an antibody specifically recognizing human CD34 antigen (a hematopoietic/vascular cell marker). (b). Similar analysis of CD34 expression in EBs (day 10) from the second GPI-AP deficient hES cell clone, AR2-c1. (c). EB-derived cells from the AR2-c1 hES cells were also stained by antibodies recognizing CD55 and CD59 (ubiquitously expressed GPI-APs), confirming the absence of GPI-APs after EB formation. (d) Assays for hematopoietic progenitor cells capable of forming colony-forming-unit granulocytes/monocytes (CFU-GM) or burst-forming-unit-erythrocyte (BFU-E). EB-derived cells in single cell suspension were plated in semi-solid methyl-cellulose media ( $10^5$  cells/plate). After 14 days, numbers of either type of colonies were counted and plotted.

Fig S4



**Figure S5. BMP4 but not TGF $\beta$  directly activates ID gene expression in human ES cells.**

Undifferentiated normal hES cells such as G-GFP were cultured on either primary mouse embryonic fibroblasts (PMEF), or Matrigel with the conditioned medium from PMEF (the feeder-free condition). The hES cells cultured under the feeder-free condition were treated with BMP4 (10 ng/ml) or TGF $\beta$  (10 ng/ml) for 24 hours. The expression of selected genes in the treated or untreated cells (mock) was quantified by real-time RT-PCR, in comparison with that in hES cells cultured on PMEF (without exogenous BMP4 or TGF $\beta$ ). Human-specific primers and probes for *NANOG* (a), *ID1* (b), *ID2* (c), *ID3* (d) and *ID4* (e) as well as for  $\beta$ -actin gene (internal control) were used for the 40-cycle PCR reaction. After normalization by the level of the  $\beta$ -actin gene, the level of target gene expression is plotted as fold relative to that in hES cells cultured on PMEF (define as 1). While the *NANOG* gene expression did not change significantly 24 hours after induction by either BMP4 or TGF $\beta$ , the expression of *ID* genes was significantly elevated by BMP4 but not TGF $\beta$ . The direct activation of *ID1* and *ID2* transcription by BMP4 was confirmed using a luciferase (Luc) reporter assay. The Luc reporter controlled by a promoter fragment of either (mouse) *Id1* gene (Xu et al., 2005) or the *Id2* gene (XH Sun, unpublished) was transfected to hES cell lines H1/G-GFP (f) or H9 (g). A  $\beta$ -galactosidase (LacZ) expression vector controlled by the EF1 $\alpha$  promoter (EF.lacZ) was also used in transfection to normalize transfection efficiency (as in Figures 6-7). Six hours of transfection, BMP4 (50 ng/ml) was added. 20 hours after, transfected cells were harvested, lysed and measured for galactosidase and luciferase activities. The relative (and LacZ-normalized) Luc activities were calculated: the mean of the *Id1*-Luc activity in the cells without BMP4 stimulation is set as 1. Mean and SD (n=4) values of both *Id1*-Luc and *Id2*-Luc in two hES cell lines were plotted.

**Fig S5** BMP4, but not TGFβ, activated gene expression of *ID1*, *ID2*, *ID3* and *ID4* in human ES cells

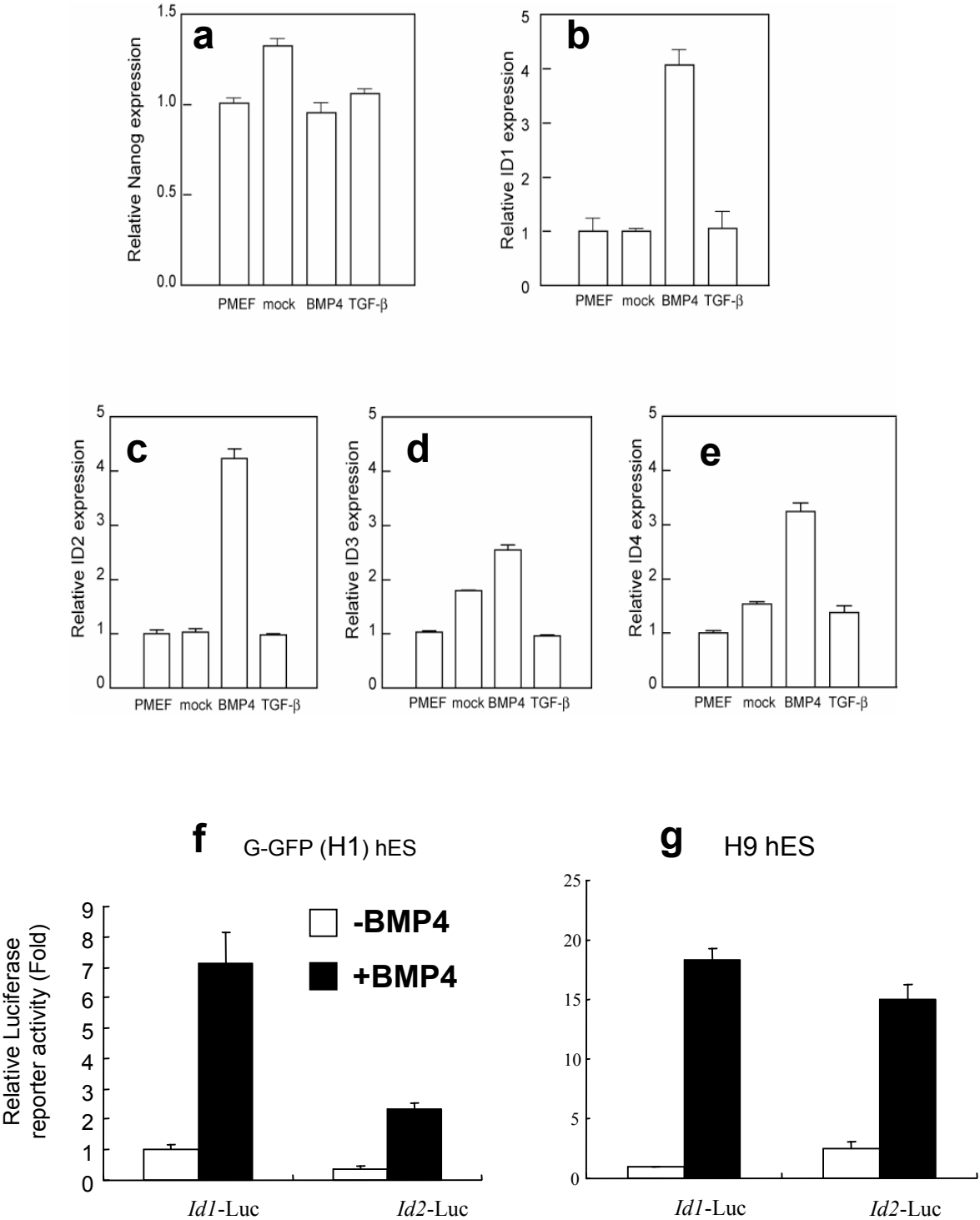


**Figure S6. NOGGIN blockade of BMP signaling during embryoid body formation**

**preferentially inhibits trophoblast differentiation from human ES cells.** Undifferentiated normal H9 hES cells were allowed to form aggregates and embryoid bodies (EB) in suspension culture in the presence of 20% FBS. Increasing concentrations of NOGGIN (up to 200 ng/ml) was added at the onset to EB formation. Culture media were replenished as needed and EBs were harvested after 10 days. The expression of selected marker genes in undifferentiated (Undiff) hES cells and EBs (in the presence or absence of NOGGIN) were measured by real-time RT-PCR as in Figure S3. The  $\beta$ -actin gene was used as an internal control as before. The expression of each marker gene in EB (in the absence of NOGGIN) was set as 1 (after the  $\beta$ -actin normalization). Mean and SD (n=4) from one of two experiments were plotted. Ten days following EB formation, *NANOG* was reduced by ~100 fold and NOGGIN addition had little effect (**a**). The expression of all the lineage differentiation markers was vastly elevated 10 days after EB formation (**b-e**). The expression of an ectoderm marker PAX6 was enhanced by added NOGGIN (**b**). However, the expression of trophectoderm/trophoblast markers CDX2 and hCGa was sharply reduced by NOGGIN (**c**). NOGGIN (up to 200 ng/ml) had a moderate effect (reduction by a half) on the upregulation of mesoderm markers CD34 and SCL/TAL-1 after EB formation (**d**). The effects of NOGGIN on endoderm marker expression were very consistent but less understood. The expression of three endoderm markers, alpha-feto-protein or AFP, GATA4, SERPINA1 (also known as alpha-1 anti-trypsin), was moderately reduced (by 8-38%) when NOGGIN at a low concentration (12.5 ng/ml) was added during EB formation (**e**). The expression of endoderm marker genes after EB formation, however, was reduced vastly when a higher concentration (100 – 200 ng/ml) of NOGGIN was used. The possibility that NOGGIN may act on additional pathways other than those of BMPs remains to be determined.

Fig S6

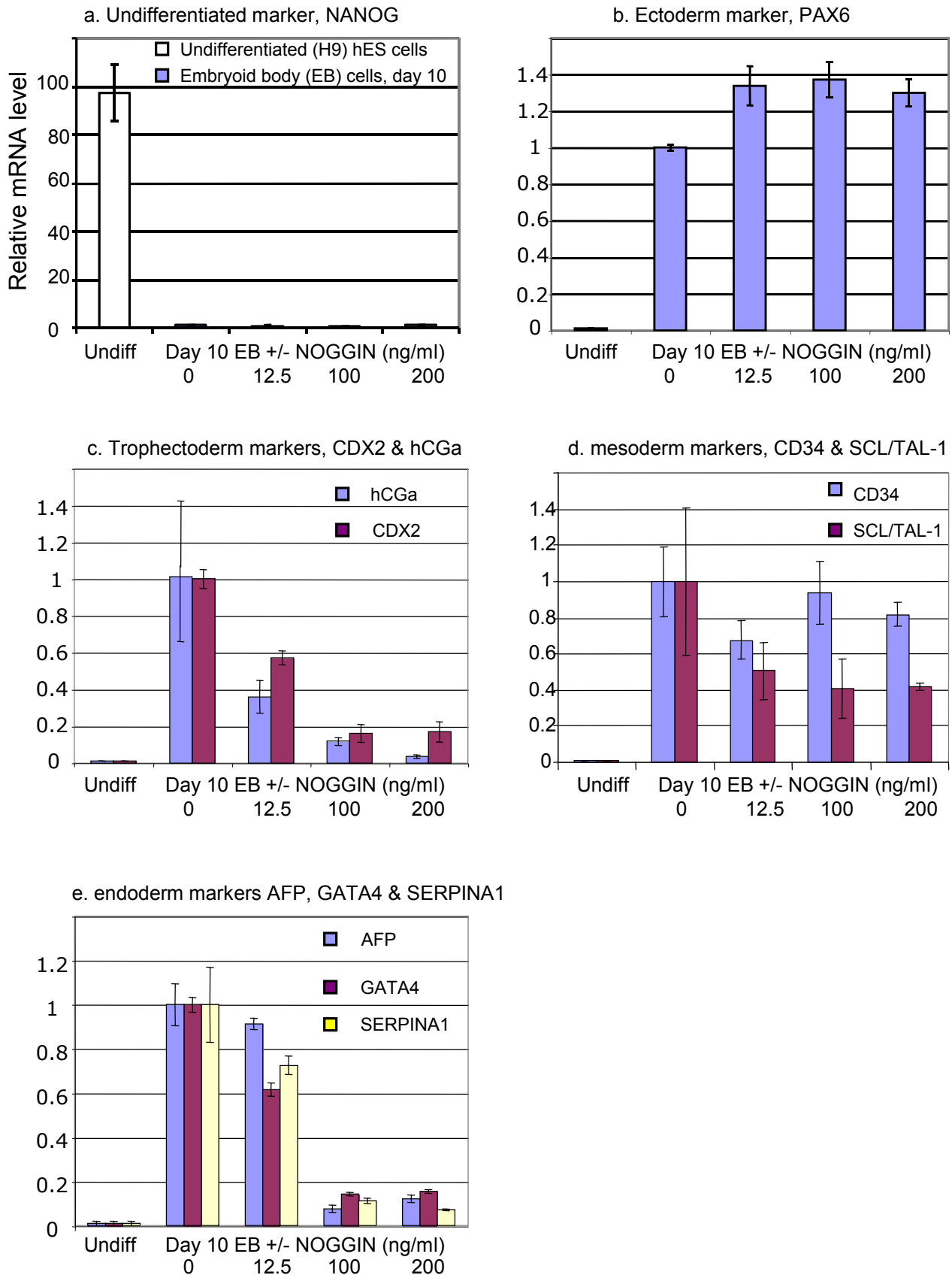




**Figure S7. Detection of DRAGON gene expression and construction of a transmembrane form of DRAGON transgene using the pDisplay expression vector.**

Human ES cells G-GFP, AR1-c1 and its derivative with an added PIG-A transgene, which all were derived from the H1 (WA01) line, and the H9 (WA09) line were used to analyze the expression of RGMa and DRAGON (also known as RGMb), two GPI-AP genes (**a**). The  $\beta$ -actin gene was used as an internal control as before, and specific primers for each gene is provided in Table S3. Consistent with the microarray data (not shown), the RGMa and DRAGON genes are abundantly expressed in both human ES cell lines. To achieve cell-surface expression of DRAGON in AR1-c1 human ES cells that are defective in PIG-A resulting in a post-translational defect for cell-surface GPI-APs, we attempted to make a novel chimeric protein using the PGGFR transmembrane domain. The encoding region of the mature portion of DRAGON (in red) devoid of the signal peptide at the N-terminus and the hydrophobic domain at the C-terminus was cloned into the pDisplay<sup>TM</sup> expression vector (Invitrogen) at Bgl II and Sac II sites (**b**). The cloned DRAGON mature form (short of the amino acids GN as compared to the predicted mature form as a GPI-AP) is fused in frame with a signal peptide, the HA and c-myc epitope tags, and the transmembrane domain. This novel cell-surface DRAGON protein/gene as a transmembrane (TM) form is dubbed as DRAGON<sup>TM</sup> (**b**). To directly confirm the cell-surface expression of DRAGON<sup>TM</sup> mediated from the pDisplay vector, we transfect the DRAGON<sup>TM</sup> or a control vector into 293T cells. Two days after, cells were harvested and stained for cell-surface expression of the tagged epitopes by antibodies specific for either HA (**c**) or c-Myc (**d**). As compared to mock transfection or by an irrelevant control vector (black lines), the DRAGON<sup>TM</sup> transfected 293T cells showed a high-level, cell-surface expression (red lines).

**Fig S7**

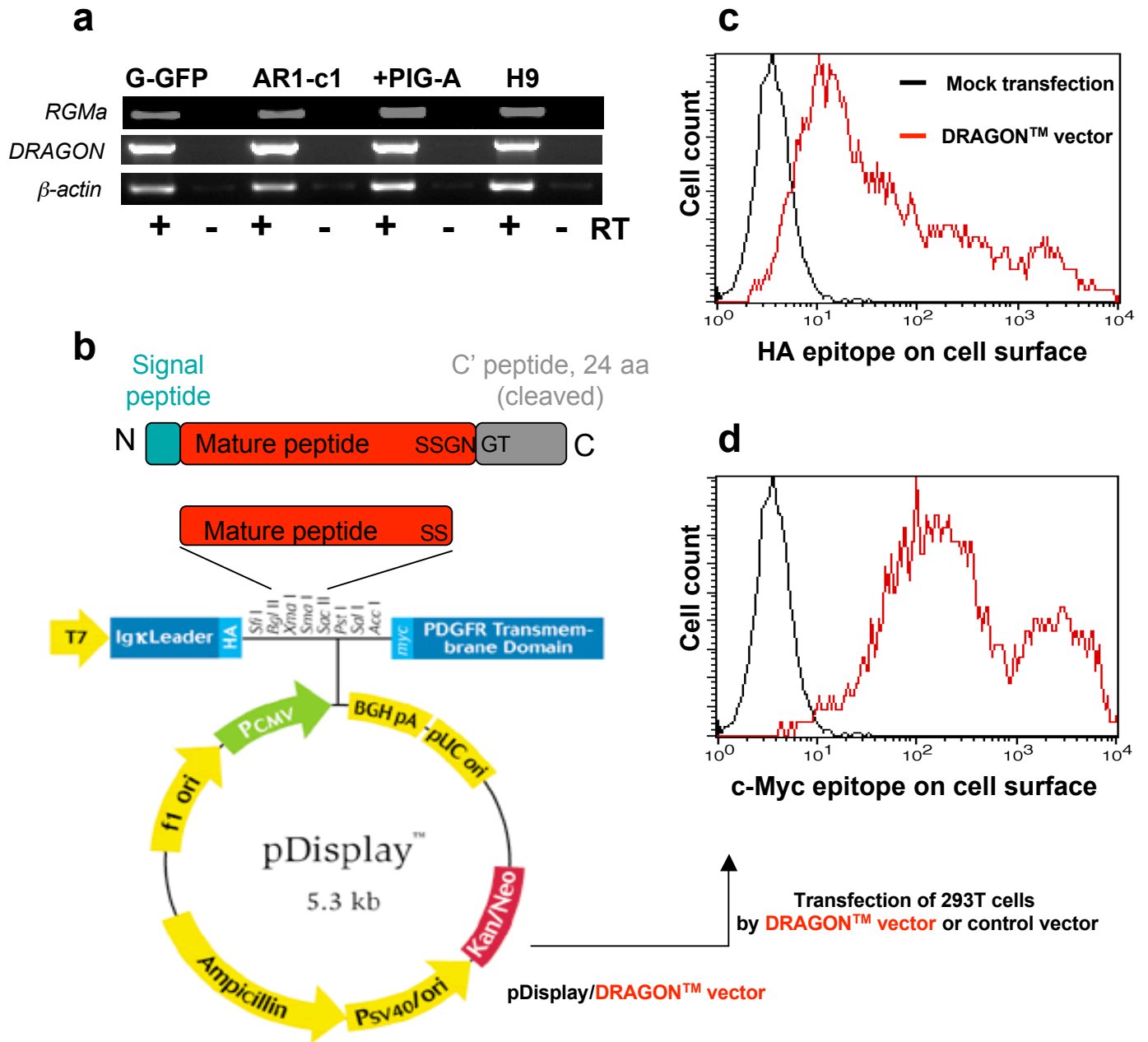


**Figure S8. Down-regulation of DRAGON gene expression in human ES cells reduces the response to BMP4 activation and the induced trophoblast formation.**

Human ES cells were transduced by various lentiviral vectors expressing a small hairpin (sh) RNA targeting RGMa, DRAGON/RGMb or HPRT1 gene (as a control). The shRNA vectors were made by The RNAi Consortium (TRC) and purchased from Sigma. After initial tests with 10 shRNA vectors targeting either RGMa or DRAGON/RGMb gene, we focused on two vectors (A3 and B3) for H9 hES cell experiments. Vector A3 (N0000130653) expresses an shRNA with a perfect match with the RGMa gene, while vector B3 (N0000137095) expressing an shRNA perfectly matched to the DRAGON/RGMb gene. An HPRT1 shRNA vector (N0000035050) is used as a control. Stably transduced hES cells were selected, based on puromycin transgene expression from the same vector. We observed little effects of the shRNA expression on the growth or phenotypes of undifferentiated hES cells. (a). Human ES cells expressing various shRNA were transfected with the *Id1*-luciferase reporter plasmid to measure BMP4 responses as in Fig 5. Six hours after transfection, cells were stimulated in the absence (-) or presence (+) of BMP4 (50 ng/ml) for 20 hours and harvested. The *Id1*-luc activity was measured, and calculated relative to the level without BMP4 stimulation (defined as 1) for each cell type. The normalized mean and SD values (n=9) were plotted. (b). RT-PCR analysis of mRNA levels of RGMa, DRAGON/RGMb and HPRT1 genes. The detected level of DRAGON/RGMb mRNA expression is always higher than that of RGMa in undifferentiated in H1 (Table S1 and Fig S7) and H9 hES cells (lanes 1). The mRNA levels of the 3 targeted genes (and  $\beta$ -actin as a control) in each type of shRNA-transduced hES cells were also measured. Lanes 2, by shRGM-A3; Lanes 3, by shRGM-B3, and Lanes 4, by HPRT1 shRNA. Supporting the data in (a), shRGM-A3 reduced RGMa mRNA level by ~3.5 fold while ShRGM-B3 reduced DRAGON/RGMb mRNA level by ~5.5 fold. (c). Significant reduction of trophoblast marker expression by shRNA targeting RGM/DRAGON. Human CG $\alpha$  gene expression in the parental H9 (lane 1) or shRNA-transduced cells (lanes 2-4) before or after BMP4 stimulation at 5 days. (c-g). Immuno-staining of a trophoblast marker TROMA-I, 5 days after BMP4 stimulation as in (c) and in Figures 6-7. In summary, BMP4-induced up-regulation of trophoblast markers such as hCG $\alpha$  and TROMA-I was significantly reduced in RGM-A3 or RGM-B3 shRNA transduced hES cells (c-g), which displayed reduced the RGM-a or RGM-b mRNA expression and the BMP4-dependent *Id1* activation (a-b).

